Version 2.61 as of April 1, 2007
Primary author: A. Haas
To be submitted to PRL

Comment to d0-run2eb-020@fnal.gov
by April 10, 2007

Search for stopped gluinos from $p\bar{p}$ collisions at $\sqrt{s} = 1.96$ TeV

V.M. Abazov,[35] B. Abbott,[75] M. Abolins,[65] B.S. Acharya,[28] M. Adams,[51] T. Adams,[49] E. Aguilo,[5] S.H. Ahn,[30] M. Ahsan,[59] G.D. Alexeev,[35] G. Alkhazov,[39] A. Alton,[64,*] G. Alverson,[63] G.A. Alves,[2] M. Anastasoaie,[34] L.S. Ancu,[34] T. Andeen,[53] S. Anderson,[45] B. Andrieu,[16] M.S. Anzelc,[53] Y. Arnoud,[13] M. Arov,[52] A. Askew,[49] B. Åsman,[40] A.C.S. Assis Jesus,[3] O. Atramentov,[49] C. Autermann,[20] C. Avila,[7] C. Ay,[23] F. Badaud,[12] A. Baden,[61] L. Bagby,[52] B. Baldin,[50] D.V. Bandurin,[59] P. Banerjee,[28] S. Banerjee,[28] E. Barberis,[63] A.-F. Barfuss,[14] P. Bargassa,[80] P. Baringer,[58] J. Barreto,[2] J.F. Bartlett,[50] U. Bassler,[16] D. Bauer,[43] S. Beale,[5] A. Bean,[58] M. Begalli,[3] M. Begel,[71] C. Belanger-Champagne,[40] L. Bellantoni,[50] A. Bellavance,[50] J.A. Benitez,[65] S.B. Beri,[26] G. Bernardi,[16] R. Bernhard,[22] L. Berntzon,[14] I. Bertram,[42] M. Besançon,[17] R. Beuselinck,[43] V.A. Bezzubov,[38] P.C. Bhat,[50] V. Bhatnagar,[26] M. Binder,[24] C. Biscarat,[19] G. Blazey,[52] F. Blekman,[43] S. Blessing,[49] D. Bloch,[18] K. Bloom,[67] A. Boehnlein,[50] D. Boline,[62] T.A. Bolton,[59] G. Borissov,[42] K. Bos,[33] T. Bose,[77] A. Brandt,[78] R. Brock,[65] G. Brooijmans,[70] A. Bross,[50] D. Brown,[78] N.J. Buchanan,[49] D. Buchholz,[53] M. Buehler,[81] V. Buescher,[21] S. Burdin,[50] S. Burke,[45] T.H. Burnett,[82] E. Busato,[16] C.P. Buszello,[43] J.M. Butler,[62] P. Calfayan,[24] S. Calvet,[14] J. Cammin,[71] S. Caron,[33] W. Carvalho,[3] B.C.K. Casey,[77] N.M. Cason,[55] H. Castilla-Valdez,[32] S. Chakrabarti,[17] D. Chakraborty,[52] K. Chan,[5] K.M. Chan,[71] A. Chandra,[48] F. Charles,[18] E. Cheu,[45] F. Chevallier,[13] D.K. Cho,[62] S. Choi,[31] B. Choudhary,[27] L. Christofek,[77] T. Christoudias,[43] S. Cihangir,[50] D. Claes,[67] B. Clément,[18] C. Clément,[40] Y. Coadou,[5] M. Cooke,[80] W.E. Cooper,[50] M. Corcoran,[80] F. Couderc,[17] M.-C. Cousinou,[14] S. Crépé-Renaudin,[13] D. Cutts,[77] M. Ćwiok,[29] H. da Motta,[2] A. Das,[62] G. Davies,[43] K. De,[78] P. de Jong,[33] S.J. de Jong,[34] E. De La Cruz-Burelo,[64] C. De Oliveira Martins,[3] J.D. Degenhardt,[64] F. Déliot,[17] M. Demarteau,[50] R. Demina,[71] D. Denisov,[50] S.P. Denisov,[38] S. Desai,[50] H.T. Diehl,[50] M. Diesburg,[50] A. Dominguez,[67] H. Dong,[72] L.V. Dudko,[37] L. Duflot,[15] S.R. Dugad,[28] D. Duggan,[49] A. Duperrin,[14] J. Dyer,[65] A. Dyshkant,[52] M. Eads,[67] D. Edmunds,[65] J. Ellison,[48] V.D. Elvira,[50] Y. Enari,[77] S. Eno,[61] P. Ermolov,[37] H. Evans,[54] A. Evdokimov,[36] V.N. Evdokimov,[38] A.V. Ferapontov,[59] T. Ferbel,[71] F. Fiedler,[24] F. Filthaut,[34] W. Fisher,[50] H.E. Fisk,[50] M. Ford,[44] M. Fortner,[52] H. Fox,[22] S. Fu,[50] S. Fuess,[50] T. Gadfort,[82] C.F. Galea,[34] E. Gallas,[50] E. Galyaev,[55] C. Garcia,[71] A. Garcia-Bellido,[82] V. Gavrilov,[36] P. Gay,[12] W. Geist,[18] D. Gelé,[18] C.E. Gerber,[51] Y. Gershtein,[49] D. Gillberg,[5] G. Ginther,[71] N. Gollub,[40] B. Gómez,[7] A. Goussiou,[55] P.D. Grannis,[72] H. Greenlee,[50] Z.D. Greenwood,[60] E.M. Gregores,[4] G. Grenier,[19] Ph. Gris,[12] J.-F. Grivaz,[15] A. Grohsjean,[24] S. Grünendahl,[50] M.W. Grünewald,[29] F. Guo,[72] J. Guo,[72] G. Gutierrez,[50] P. Gutierrez,[75] A. Haas,[70] N.J. Hadley,[61] P. Haefner,[24] S. Hagopian,[49] J. Haley,[68] I. Hall,[75] R.E. Hall,[47] L. Han,[6] K. Hanagaki,[50] P. Hansson,[40] K. Harder,[44] A. Harel,[71] R. Harrington,[63] J.M. Hauptman,[57] R. Hauser,[65] J. Hays,[43] T. Hebbeker,[20] D. Hedin,[52] J.G. Hegeman,[33] J.M. Heinmiller,[51] A.P. Heinson,[48] U. Heintz,[62] C. Hensel,[58] K. Herner,[72] G. Hesketh,[63] M.D. Hildreth,[55] R. Hirosky,[81] J.D. Hobbs,[72] B. Hoeneisen,[11] H. Hoeth,[25] M. Hohlfeld,[15] S.J. Hong,[30] R. Hooper,[77] P. Houben,[33] Y. Hu,[72] Z. Hubacek,[9] V. Hynek,[8] I. Iashvili,[69] R. Illingworth,[50] A.S. Ito,[50] S. Jabeen,[62] M. Jaffré,[15] S. Jain,[75] K. Jakobs,[22] C. Jarvis,[61] R. Jesik,[43] K. Johns,[45] C. Johnson,[70] M. Johnson,[50] A. Jonckheere,[50] P. Jonsson,[43] A. Juste,[50] D. Käfer,[20] S. Kahn,[73] E. Kajfasz,[14] A.M. Kalinin,[35] J.M. Kalk,[60] J.R. Kalk,[65] S. Kappler,[20] D. Karmanov,[37] J. Kasper,[62] P. Kasper,[50] I. Katsanos,[70] D. Kau,[49] R. Kaur,[26] V. Kaushik,[78] R. Kehoe,[79] S. Kermiche,[14] N. Khalatyan,[38] A. Khanov,[76] A. Kharchilava,[69] Y.M. Kharzheev,[35] D. Khatidze,[70] H. Kim,[31] T.J. Kim,[30] M.H. Kirby,[34] B. Klima,[50] J.M. Kohli,[26] J.-P. Konrath,[22] M. Kopal,[75] V.M. Korablev,[38] J. Kotcher,[73] B. Kothari,[70] A. Koubarovsky,[37] A.V. Kozelov,[38] D. Krop,[54] A. Kryemadhi,[81] T. Kuhl,[23] A. Kumar,[69] S. Kunori,[61] A. Kupco,[10] T. Kurča,[19] J. Kvita,[8] D. Lam,[55] S. Lammers,[70] G. Landsberg,[77] J. Lazoflores,[49] P. Lebrun,[19] W.M. Lee,[50] A. Leflat,[37] F. Lehner,[41] V. Lesne,[12] J. Leveque,[45] P. Lewis,[43] J. Li,[78] L. Li,[48] Q.Z. Li,[50] S.M. Lietti,[4] J.G.R. Lima,[52] D. Lincoln,[50] J. Linnemann,[65] V.V. Lipaev,[38] R. Lipton,[50] Z. Liu,[5] L. Lobo,[43] A. Lobodenko,[39] M. Lokajicek,[10] A. Lounis,[18] P. Love,[42] H.J. Lubatti,[82] M. Lynker,[55] A.L. Lyon,[50] A.K.A. Maciel,[2] R.J. Madaras,[46] P. Mättig,[25] C. Magass,[20] A. Magerkurth,[64] N. Makovec,[15] P.K. Mal,[55] H.B. Malbouisson,[3] S. Malik,[67] V.L. Malyshev,[35] H.S. Mao,[50] Y. Maravin,[59] B. Martin,[13] R. McCarthy,[72] A. Melnitchouk,[66] A. Mendes,[14] L. Mendoza,[7] P.G. Mercadante,[4] M. Merkin,[37] K.W. Merritt,[50] A. Meyer,[20] J. Meyer,[21] M. Michaut,[17] H. Miettinen,[80] T. Millet,[19] J. Mitrevski,[70] J. Molina,[3] R.K. Mommsen,[44] N.K. Mondal,[28] J. Monk,[44]

R.W. Moore,[5] T. Moulik,[58] G.S. Muanza,[19] M. Mulders,[50] M. Mulhearn,[70] O. Mundal,[21] L. Mundim,[3] E. Nagy,[14] M. Naimuddin,[50] M. Narain,[77] N.A. Naumann,[34] H.A. Neal,[64] J.P. Negret,[7] P. Neustroev,[39] H. Nilsen,[22] C. Noeding,[22] A. Nomerotski,[50] S.F. Novaes,[4] T. Nunnemann,[24] V. O'Dell,[50] D.C. O'Neil,[5] G. Obrant,[39] C. Ochando,[15] V. Oguri,[3] N. Oliveira,[3] D. Onoprienko,[59] N. Oshima,[50] J. Osta,[55] R. Otec,[9] G.J. Otero y Garzón,[51] M. Owen,[44] P. Padley,[80] M. Pangilinan,[77] N. Parashar,[56] S.-J. Park,[71] S.K. Park,[30] J. Parsons,[70] R. Partridge,[77] N. Parua,[54] A. Patwa,[73] G. Pawloski,[80] P.M. Perea,[48] K. Peters,[44] Y. Peters,[25] P. Pétroff,[15] M. Petteni,[43] R. Piegaia,[1] J. Piper,[65] M.-A. Pleier,[21] P.L.M. Podesta-Lerma,[32,§] V.M. Podstavkov,[50] Y. Pogorelov,[55] M.-E. Pol,[2] A. Pompoš,[75] B.G. Pope,[65] A.V. Popov,[38] C. Potter,[5] W.L. Prado da Silva,[3] H.B. Prosper,[49] S. Protopopescu,[73] J. Qian,[64] A. Quadt,[21] B. Quinn,[66] M.S. Rangel,[2] K.J. Rani,[28] K. Ranjan,[27] P.N. Ratoff,[42] P. Renkel,[79] S. Reucroft,[63] P. Rich,[44] M. Rijssenbeek,[72] I. Ripp-Baudot,[18] F. Rizatdinova,[76] S. Robinson,[43] R.F. Rodrigues,[3] C. Royon,[17] P. Rubinov,[50] R. Ruchti,[55] G. Sajot,[13] A. Sánchez-Hernández,[32] M.P. Sanders,[16] A. Santoro,[3] G. Savage,[50] L. Sawyer,[60] T. Scanlon,[43] D. Schaile,[24] R.D. Schamberger,[72] Y. Scheglov,[39] H. Schellman,[53] P. Schieferdecker,[24] C. Schmitt,[25] C. Schwanenberger,[44] A. Schwartzman,[68] R. Schwienhorst,[65] J. Sekaric,[49] S. Sengupta,[49] H. Severini,[75] E. Shabalina,[51] M. Shamim,[59] V. Shary,[17] A.A. Shchukin,[38] R.K. Shivpuri,[27] D. Shpakov,[50] V. Siccardi,[18] R.A. Sidwell,[59] V. Simak,[9] V. Sirotenko,[50] P. Skubic,[75] P. Slattery,[71] D. Smirnov,[55] R.P. Smith,[50] G.R. Snow,[67] J. Snow,[74] S. Snyder,[73] S. Söldner-Rembold,[44] L. Sonnenschein,[16] A. Sopczak,[42] M. Sosebee,[78] K. Soustruznik,[8] M. Souza,[2] B. Spurlock,[78] J. Stark,[13] J. Steele,[60] V. Stolin,[36] A. Stone,[51] D.A. Stoyanova,[38] J. Strandberg,[64] S. Strandberg,[40] M.A. Strang,[69] M. Strauss,[75] R. Ströhmer,[24] D. Strom,[53] M. Strovink,[46] L. Stutte,[50] S. Sumowidagdo,[49] P. Svoisky,[55] A. Sznajder,[3] M. Talby,[14] P. Tamburello,[45] A. Tanasijczuk,[1] W. Taylor,[5] P. Telford,[44] J. Temple,[45] B. Tiller,[24] F. Tissandier,[12] M. Titov,[17] V.V. Tokmenin,[35] M. Tomoto,[50] T. Toole,[61] I. Torchiani,[22] T. Trefzger,[23] S. Trincaz-Duvoid,[16] D. Tsybychev,[72] B. Tuchming,[17] C. Tully,[68] P.M. Tuts,[70] R. Unalan,[65] L. Uvarov,[39] S. Uvarov,[39] S. Uzunyan,[52] B. Vachon,[5] P.J. van den Berg,[33] B. van Eijk,[35] R. Van Kooten,[54] W.M. van Leeuwen,[33] N. Varelas,[51] E.W. Varnes,[45] A. Vartapetian,[78] I.A. Vasilyev,[38] M. Vaupel,[25] P. Verdier,[19] L.S. Vertogradov,[35] M. Verzocchi,[50] F. Villeneuve-Seguier,[43] P. Vint,[43] J.-R. Vlimant,[16] E. Von Toerne,[59] M. Voutilainen,[67,‡] M. Vreeswijk,[33] H.D. Wahl,[49] L. Wang,[61] M.H.L.S Wang,[50] J. Warchol,[55] G. Watts,[82] M. Wayne,[55] G. Weber,[23] M. Weber,[50] H. Weerts,[65] A. Wenger,[22,#] N. Wermes,[21] M. Wetstein,[61] A. White,[78] D. Wicke,[25] G.W. Wilson,[58] S.J. Wimpenny,[48] M. Wobisch,[50] D.R. Wood,[63] T.R. Wyatt,[44] Y. Xie,[77] S. Yacoob,[53] R. Yamada,[50] M. Yan,[61] T. Yasuda,[50] Y.A. Yatsunenko,[35] K. Yip,[73] H.D. Yoo,[77] S.W. Youn,[53] C. Yu,[13] J. Yu,[78] A. Yurkewicz,[72] A. Zatserklyaniy,[52] C. Zeitnitz,[25] D. Zhang,[50] T. Zhao,[82] B. Zhou,[64] J. Zhu,[72] M. Zielinski,[71] D. Zieminska,[54] A. Zieminski,[54] V. Zutshi,[52] and E.G. Zverev[37]

(DØ Collaboration)

[1] *Universidad de Buenos Aires, Buenos Aires, Argentina*
[2] *LAFEX, Centro Brasileiro de Pesquisas Físicas, Rio de Janeiro, Brazil*
[3] *Universidade do Estado do Rio de Janeiro, Rio de Janeiro, Brazil*
[4] *Instituto de Física Teórica, Universidade Estadual Paulista, São Paulo, Brazil*
[5] *University of Alberta, Edmonton, Alberta, Canada, Simon Fraser University, Burnaby, British Columbia, Canada, York University, Toronto, Ontario, Canada, and McGill University, Montreal, Quebec, Canada*
[6] *University of Science and Technology of China, Hefei, People's Republic of China*
[7] *Universidad de los Andes, Bogotá, Colombia*
[8] *Center for Particle Physics, Charles University, Prague, Czech Republic*
[9] *Czech Technical University, Prague, Czech Republic*
[10] *Center for Particle Physics, Institute of Physics, Academy of Sciences of the Czech Republic, Prague, Czech Republic*
[11] *Universidad San Francisco de Quito, Quito, Ecuador*
[12] *Laboratoire de Physique Corpusculaire, IN2P3-CNRS, Université Blaise Pascal, Clermont-Ferrand, France*
[13] *Laboratoire de Physique Subatomique et de Cosmologie, IN2P3-CNRS, Universite de Grenoble 1, Grenoble, France*
[14] *CPPM, IN2P3-CNRS, Université de la Méditerranée, Marseille, France*
[15] *Laboratoire de l'Accélérateur Linéaire, IN2P3-CNRS et Université Paris-Sud, Orsay, France*
[16] *LPNHE, IN2P3-CNRS, Universités Paris VI and VII, Paris, France*
[17] *DAPNIA/Service de Physique des Particules, CEA, Saclay, France*
[18] *IPHC, IN2P3-CNRS, Université Louis Pasteur, Strasbourg, France, and Université de Haute Alsace, Mulhouse, France*
[19] *IPNL, Université Lyon 1, CNRS/IN2P3, Villeurbanne, France and Université de Lyon, Lyon, France*
[20] *III. Physikalisches Institut A, RWTH Aachen, Aachen, Germany*
[21] *Physikalisches Institut, Universität Bonn, Bonn, Germany*
[22] *Physikalisches Institut, Universität Freiburg, Freiburg, Germany*
[23] *Institut für Physik, Universität Mainz, Mainz, Germany*
[24] *Ludwig-Maximilians-Universität München, München, Germany*
[25] *Fachbereich Physik, University of Wuppertal, Wuppertal, Germany*

[26] *Panjab University, Chandigarh, India*
[27] *Delhi University, Delhi, India*
[28] *Tata Institute of Fundamental Research, Mumbai, India*
[29] *University College Dublin, Dublin, Ireland*
[30] *Korea Detector Laboratory, Korea University, Seoul, Korea*
[31] *SungKyunKwan University, Suwon, Korea*
[32] *CINVESTAV, Mexico City, Mexico*
[33] *FOM-Institute NIKHEF and University of Amsterdam/NIKHEF, Amsterdam, The Netherlands*
[34] *Radboud University Nijmegen/NIKHEF, Nijmegen, The Netherlands*
[35] *Joint Institute for Nuclear Research, Dubna, Russia*
[36] *Institute for Theoretical and Experimental Physics, Moscow, Russia*
[37] *Moscow State University, Moscow, Russia*
[38] *Institute for High Energy Physics, Protvino, Russia*
[39] *Petersburg Nuclear Physics Institute, St. Petersburg, Russia*
[40] *Lund University, Lund, Sweden, Royal Institute of Technology and Stockholm University, Stockholm, Sweden, and Uppsala University, Uppsala, Sweden*
[41] *Physik Institut der Universität Zürich, Zürich, Switzerland*
[42] *Lancaster University, Lancaster, United Kingdom*
[43] *Imperial College, London, United Kingdom*
[44] *University of Manchester, Manchester, United Kingdom*
[45] *University of Arizona, Tucson, Arizona 85721, USA*
[46] *Lawrence Berkeley National Laboratory and University of California, Berkeley, California 94720, USA*
[47] *California State University, Fresno, California 93740, USA*
[48] *University of California, Riverside, California 92521, USA*
[49] *Florida State University, Tallahassee, Florida 32306, USA*
[50] *Fermi National Accelerator Laboratory, Batavia, Illinois 60510, USA*
[51] *University of Illinois at Chicago, Chicago, Illinois 60607, USA*
[52] *Northern Illinois University, DeKalb, Illinois 60115, USA*
[53] *Northwestern University, Evanston, Illinois 60208, USA*
[54] *Indiana University, Bloomington, Indiana 47405, USA*
[55] *University of Notre Dame, Notre Dame, Indiana 46556, USA*
[56] *Purdue University Calumet, Hammond, Indiana 46323, USA*
[57] *Iowa State University, Ames, Iowa 50011, USA*
[58] *University of Kansas, Lawrence, Kansas 66045, USA*
[59] *Kansas State University, Manhattan, Kansas 66506, USA*
[60] *Louisiana Tech University, Ruston, Louisiana 71272, USA*
[61] *University of Maryland, College Park, Maryland 20742, USA*
[62] *Boston University, Boston, Massachusetts 02215, USA*
[63] *Northeastern University, Boston, Massachusetts 02115, USA*
[64] *University of Michigan, Ann Arbor, Michigan 48109, USA*
[65] *Michigan State University, East Lansing, Michigan 48824, USA*
[66] *University of Mississippi, University, Mississippi 38677, USA*
[67] *University of Nebraska, Lincoln, Nebraska 68588, USA*
[68] *Princeton University, Princeton, New Jersey 08544, USA*
[69] *State University of New York, Buffalo, New York 14260, USA*
[70] *Columbia University, New York, New York 10027, USA*
[71] *University of Rochester, Rochester, New York 14627, USA*
[72] *State University of New York, Stony Brook, New York 11794, USA*
[73] *Brookhaven National Laboratory, Upton, New York 11973, USA*
[74] *Langston University, Langston, Oklahoma 73050, USA*
[75] *University of Oklahoma, Norman, Oklahoma 73019, USA*
[76] *Oklahoma State University, Stillwater, Oklahoma 74078, USA*
[77] *Brown University, Providence, Rhode Island 02912, USA*
[78] *University of Texas, Arlington, Texas 76019, USA*
[79] *Southern Methodist University, Dallas, Texas 75275, USA*
[80] *Rice University, Houston, Texas 77005, USA*
[81] *University of Virginia, Charlottesville, Virginia 22901, USA*
[82] *University of Washington, Seattle, Washington 98195, USA*

(Dated: April 1, 2007)

A long-lived, colored, heavy particle is predicted in several models of beyond the standard model physics, one example being the gluino ($\tilde{g}$) in split supersymmetry. Gluinos carry color charge and are thus expected to hadronize, if long lived, into colorless bound states called R-hadrons. Some

fraction of the R-hadrons can become charged and lose enough momentum through ionization to come to rest in dense particle detectors. Approximately 410 pb^{-1} of $p\bar{p}$ collisions at $\sqrt{s} = 1.96$ TeV collected with the D0 detector during Run II of the Fermilab Tevatron collider is analyzed in search of such "stopped gluinos" ($\tilde{G}$) decaying into a gluon and a neutralino (χ_1^0), reconstructed as a jet and missing energy. No excess is observed above the expected background from cosmic muons, and limits are placed on the (gluino cross section) × (probability to stop) × [BR($\tilde{G}\to g\chi_1^0$)] as a function of the gluino and χ_1^0 masses, for gluino lifetimes from 30 μs – 100 hours.

PACS numbers:

Split supersymmetry is a relatively new variant of supersymmetry, in which the supersymmetric scalars are heavy (possibly GUT-scale) compared to the (SUSY) fermions [1]. Due to the scalars' high masses, gluino decays are suppressed, and it can be long-lived. The gluinos hadronize into "R-hadrons" [2], colorless bound states of a gluino and other quarks or gluons. At the Tevatron, gluinos could be pair produced through strong interactions. If $M_{\rm SUSY} > 10^6$ GeV, the R-hadrons live long enough (>10 ns) to reach the D0 calorimeters. As studied in Ref. [3], some charged R-hadrons can become such "stopped gluinos" by losing all of their momentum through ionization and coming to rest in surrounding dense material.

About 410 pb^{-1} of data taken with the D0 detector [4] from November 2002 – August 2004 were reconstructed and analyzed in search of stopped gluinos. The D0 detector has a magnetic central tracking system surrounded by a uranium/liquid-argon calorimeter, contained within a muon spectrometer. The tracking system consists of a silicon microstrip tracker (SMT) and a central fiber tracker (CFT), both located within a 2 T solenoidal magnet. The SMT and CFT have designs optimized for tracking and vertexing at pseudorapidities $|\eta| < 2.5$, where $\eta = -\ln[\tan(\theta/2)]$, and θ is the polar angle with respect to the proton beam direction (z). The calorimeter has a central section (CC) covering up to $|\eta| \approx 1.1$, and two end calorimeters (EC) extending coverage to $|\eta| \approx 4.2$, all housed in separate cryostats [5]. The calorimeter is divided into an electromagnetic part followed by fine and coarse hadronic sections. Scintillators between the CC and EC cryostats provide additional sampling of developing showers for $1.1 < |\eta| < 1.4$. The muon system consists of a layer of tracking detectors and scintillation trigger counters in front of 1.8 T toroidal magnets (the A layer), followed by two similar layers behind the toroids (the B and C layers), which provide muon tracking for $|\eta| < 2$. The luminosity is measured using scintillator arrays located in front of the EC cryostats, covering $2.7 < |\eta| < 4.4$. The trigger system comprises three levels (L1, L2, and L3), each performing an increasingly detailed event reconstruction in order to select the events of interest.

For this analysis, we search for stopped gluinos decaying into a gluon and a neutralino. The gluino lifetime is assumed to be long enough such that the decay occurs during an accelerator bunch crossing later than the one that produced it. For the L1 trigger to be live again during the decay, this lifetime must be at least 30 μs. The efficiency for recording the gluino decay is modeled as a function of the gluino lifetime, up to a lifetime of 100 hours. When the decay occurs during a bunch crossing with very little other high-p_T activity, the signal signature is a largely empty event with a single high-energy deposit in the calorimeter, reconstructed as a jet and large missing transverse energy ($\not\!\!E_T$).

Since no $p\bar{p}$ interaction is expected to be correlated with the stopped gluino decay, the trigger for each event requires that neither of the luminosity scintillator arrays fired. At least two calorimeter towers of size $\eta \times \phi$=0.2×0.2 with E_T>3 GeV are also required at L1, where ϕ is the azimuthal angle around the beamline. A reconstructed jet with E_T>15 GeV is required at L3. Jets are reconstructed with the Run II Improved Legacy Cone Algorithm [6] with a cone of radius 0.5 in $\eta \times \phi$ space. Loose cuts are used to select a data sample to study. We require exactly one jet in the event with E>90 GeV, and no other jets with E_T>8 GeV. This threshold is high enough such that the calorimeter part of the trigger is nearly 100% efficient.

To simulate the jets that would be produced by stopped gluino decays, the PYTHIA [7] event generator is used to produce Z+gluon events, with the Z boson forced to decay to neutrinos. The location of the interaction point is placed inside the calorimeter, and events are further weighted such that the final decay position distribution is that expected for stopped gluinos. The radial location of the gluino when it decays depends on the way gluinos lose energy via ionization and stop in the calorimeters. This calculation was performed [3] for a distribution of material similar to that of the D0 calorimeters and a gluino velocity distribution as expected from production at the Tevatron. The η distribution is determined by the fact that gluinos would tend to be produced near threshold at the Tevatron, and that only slow gluinos would stop. The gluinos are thus expected to be distributed proportionally to $\sin\theta$. More than 75% of gluinos that stop have $|\eta|$<1. Initial-state radiation is turned off in PYTHIA as are multiple parton interactions. The spectator particles coming from the rest of the $p\bar{p}$ interaction, such as the underlying event, are removed at the generator stage by removing all far-forward particles

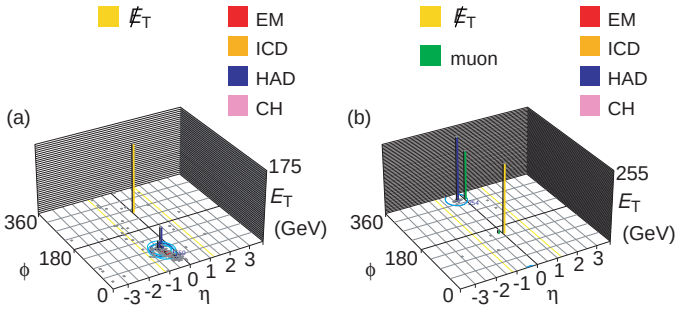

FIG. 1: a) A simulated stopped gluino decay event, for $M_{\tilde{g}}$=400 GeV. b) A typical cosmic muon, hard Bremsstrahlung, shower. The height of each bar corresponds to the total E_T in that $\eta \times \phi$ calorimeter tower. The $\not\!\!E_T$ is shown as a yellow bar and reconstructed muons are shown in green (color online).

with $|p_z/E| > 0.95$. Because the gluinos are at rest and randomly oriented in space when they decay, the gluon is emitted in a random direction. Thus a random 3D rotation is applied to the remaining simulated particles.

The energy of the gluon, which hadronizes and fragments into a jet, depends on the gluino and neutralino masses:

$$E = (M_{\tilde{g}}^2 - M_{\chi_1^0}^2)/2M_{\tilde{g}}. \quad (1)$$

Simulated jets are corrected for relative differences between the data and simulation jet energy scales. The calorimeter electronics sample the shaped ionization signal only once per bunch crossing, at the assumed peak of the signal for jets originating from a $p\bar{p}$ interaction, but the gluino decay can occur at any time with respect to a bunch crossing. So jet energies in the simulation are also corrected (downwards) according to a model of this "out-of-time" calorimeter response. The average degradation of energy is 30%, although more than half of the jets are not significantly degraded.

We generate four samples of stopped gluinos, containing about 1000 events each, using a GEANT-based [8] detector simulation and reconstructed using the same algorithms as data. They correspond to gluino masses of 200, 300, 400, and 500 GeV, with a neutralino mass of 90 GeV. Using Eq. 1, we note that these samples thus correspond to generated gluon energies of 80, 137, 190, and 242 GeV, respectively. An event display of a simulated stopped gluino decay is shown in Fig. 1(a).

The primary source of background is cosmic muons, which are able to fake a gluino signal if they initiate a high-energy shower within the calorimeter. Hard Bremsstrahlung emission is responsible for the majority of the showers. These showers tend to be very narrow, since they are electromagnetic in nature and thus have small interaction lengths compared to hadronic showers. Most of the energy is deposited in a few calorimeter towers, see Fig. 1(b). However, sometimes a wide, hadronic-like, shower can be created either due to real deep-inelastic scattering, fluctuations of the shower, or detector effects.

Cosmic muons can usually be identified by the presence of a high-energy muon, either entering or exiting the detector, using the muon detectors. In particular, a coincidence of muon hits in the outer two layers of the muon system, behind the thick iron toroid magnet, are very strong evidence of a muon. The inner-layer muon hits are often also caused by the signal, due to particles escaping the calorimeters, so are difficult to use for background rejection. Sometimes the muon is not detected, due to detector inefficiencies or the limited detector acceptance, only for $|\eta|<2$. Muons can also be detected, in principle, through their ionizing interactions in the calorimeter, where they are a minimum-ionizing particle (MIP). However, these MIP trails are difficult to identify in this geometry where the direction of the muon path is unknown, and also there is a large shower nearby which overlaps with the energy deposited by the MIP.

Another source of background events is beam-halo muons, or "beam-muons." These are real muons, in-time with the $p\bar{p}$ bunch crossings, and traveling nearly parallel to the beam. Often, a muon scintillator hit or two can be associated with the muon, and the muon is measured to be within $\Delta t<10$ ns of a bunch crossing. Another feature of the beam-muons is that they are nearly all in the plane of the accelerator beam, i.e. with ϕ very near to an integer multiple of π. Beam-muon showers are also typically very narrow in ϕ.

Since the trigger requires no firing of the luminosity scintillator arrays, nearly all of the $p\bar{p}$ beam produced backgrounds are eliminated. An exception is diffractive events with forward rapidity gaps in both the positive and negative η regions. However, after requiring no primary vertex (PV) to be reconstructed and large $\not\!\!E_T$ (implicit from the requirement of a single high-energy jet), these events are eliminated. Dijet events in the same data sample are studied to understand the $\not\!\!E_T$ spectrum and PV reconstruction efficiency for beam-related backgrounds. Other small sources of physics background considered are cosmic neutrons and neutrinos, both of which are found to be negligible.

Finally, since the signal process is rare, we also consider occasional fake signal processes caused by detector problems. We require the jet to be in $|\eta|<0.9$, since the forward regions of the calorimeter are observed to have more frequent (yet still rare) detector problems. Also, the gluino signal tends to be concentrated in the central detector region. Remaining problems are isolated to a specific set of runs, detector region, or both, and such events are easily removed.

Given the background characteristics, the following criteria are used to select events containing "wide-showers": jet η-width and ϕ-width >0.08 and jet $n_{90} \geq 10$, where n_{90} is the smallest number of calorimeter towers in the

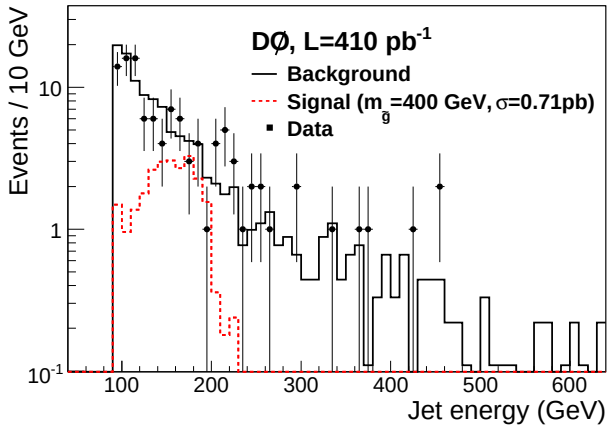

FIG. 2: A comparison of the wide-shower no-muon data (points) to the expected background (solid histogram) with logarithmic scale. Also shown is the simulated signal for $M_{\tilde{g}}$=400 GeV and $M_{\chi_1^0}$=90 GeV at the excluded production cross section limit of 0.71 pb (dashed histogram).

jet that make up 90% of the jet energy. The reverse criteria define a "narrow-shower." Criteria are also defined which select events containing "no-muon" or a "cosmic-muon." An event contains no-muon if there are no B-C layer muon segments in the event, and no A layer segments with $\Delta\phi$>1.5 radians from the jet direction. Cosmic-muon events have at least one B-C layer muon segment with $|\Delta t|$>10 ns from the bunch crossing time. A candidate stopped gluino decay event contains both a wide-shower and no-muon.

To estimate the number of such wide-shower no-muon events expected from background, we use the assumption that the probability not to reconstruct the cosmic muon in the muon system is independent of whether the muon's shower in the calorimeter is narrow or wide. We first measure the probability to not reconstruct the muon ($P_{\rm nomu}$) in the narrow-shower cosmic-muon data sample, and determine $P_{\rm nomu}$=0.11±0.01, independent of jet energy. This probability is then applied to the wide-shower cosmic-muon data sample to predict the jet energy spectrum of wide-shower no-muon background events, as shown in Fig. 2 along with the observed wide-shower no-muon events in data. The data agree with the estimated background, and there is no significant excess of data in any jet energy range.

We search for a signal in jet energy ranges with sizes chosen from the jet energy resolutions of the simulated samples. The ranges are from $M-\sigma/2$ to $M+2\sigma$, where M is the mean jet energy of the sample and σ is the sample's jet energy RMS after all selections and corrections. Approximately 80% of the simulated signal events are within this window cut, depending weakly on the signal mass. An asymmetric window is chosen since the background is falling exponentially with increasing jet energy.

TABLE I: The data, background, signal efficiency, and expected and observed cross section upper limits (at the 95% C.L.) for each jet energy range, for a small gluino lifetime, less than 3 hours.

Energy (GeV)	Data	Bgnd.	Eff.	Exp. (pb)	Obs. (pb)
92.5–104.6	30	37.07	0.017	2.61	1.81
112.4–156.6	39	40.26	0.049	0.94	0.89
141.3–213.0	34	30.91	0.068	0.56	0.71
168.7–270.6	32	25.74	0.072	0.48	0.75

To first order, the detection efficiency for the decays of the stopped gluino signal events can be estimated from the simulation, but some effects are not modeled. There is a loss of efficiency at the trigger level from the requirement of neither luminosity scintillator array firing. If a minimum bias collision happens to occur during the bunch crossing when the gluino decays, a luminosity scintillator array may fire. The fraction of the time this occurs has been measured using cosmic-muon events triggered on a jet-only trigger with higher threshold. The efficiency of the luminosity scintillator array trigger requirement, averaged over the data set, is 75%. The probability to have minimum bias interactions during a given crossing is Poisson distributed, with a mean proportional to the instantaneous luminosity. A detailed model of the trigger efficiency is made as a function of the gluino lifetime, for lifetimes up to 100 hours, using the typical Tevatron store luminosity profile as an input. Another source of inefficiency is that the trigger is not live all the time, but only during the "live super-bunches," which make up 68% of the total run time, with minimal uncertainty.

The uncertainties from all sources which affect the signal acceptance are added in quadrature, totaling (20–25)%. They include the modeling of the out-of-time jet response (12%), the data/simulation jet energy scale (9%), the η and radial distributions of stopped gluinos [(7–9)%], other geometrical or kinematic acceptances (5%), and trigger efficiency [(5–15)%].

Given an observed number of candidate events, an expected number of background events, and a signal efficiency in a certain jet energy range, we can exclude at the 95% C.L. a calculated rate of signal events giving jets of that energy, taking systematic uncertainties into account. This is a fairly model-independent result, limiting the rate of any out-of-time mono-jet signal of a given energy. Table I shows the observed and expected cross section limits, for a small gluino lifetime, less than 3 hours.

From the relation between the gluino and χ_1^0 masses and the observed jet energy, Eq. 1, one can solve for the gluino mass and results can be translated from the generated set of signal samples to any other set of ($M_{\tilde{g}}$,$M_{\chi_1^0}$) which would give the same jet energy. We can therefore place upper limits on the stopped gluino cross section

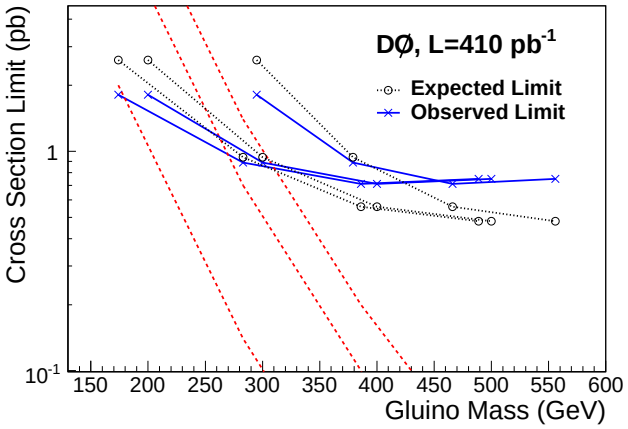

FIG. 3: The 95% C.L. expected (dotted line, circles) and observed (solid line, crosses) upper limits on the cross section of stopped gluinos, assuming a 100% BR of $\tilde{G}\to g\chi_1^0$ and a small gluino lifetime (<3 hours), for three choices of the simulated χ_1^0 mass: 50, 90 and 200 GeV, from left to right. Also shown is the theoretical cross section (dashed line), from Ref. [3], for conversion cross sections of 0.3, 3, and 30 mb (left to right).

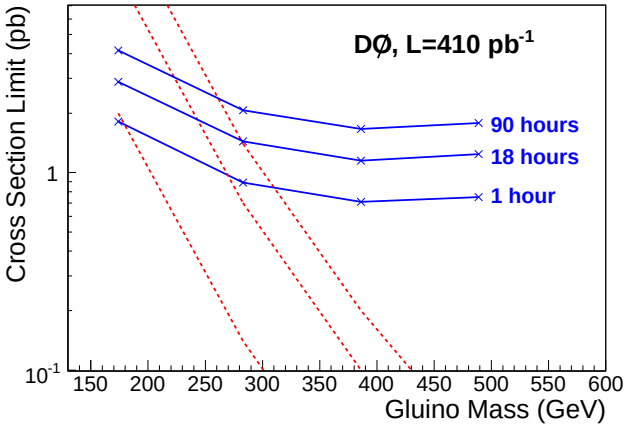

FIG. 4: The 95% C.L. upper limits observed on the cross section of stopped gluinos (solid line, crosses), assuming a 100% BR of $\tilde{G}\to g\chi_1^0$, for various assumptions of the gluino lifetime: 1, 18, and 90 hours, for a χ_1^0 mass of 50 GeV. Also shown is the theoretical cross section (dashed line), from Ref. [3], for conversion cross sections of 0.3, 3, and 30 mb (left to right).

vs. the gluino mass, for an assumed χ_1^0 mass, assuming a 100% branching fraction for $\tilde{G}\to g\chi_1^0$. These can be compared with the predicted cross sections for stopped gluinos (which include its production rate and its probability to stop) taken from Ref. [3]. Three curves are drawn to represent the large theory uncertainty, resulting from the variation of the neutral to charged R-hadron conversion cross section used. Fig. 3 shows these upper limits for assumed χ_1^0 masses of 50, 90, and 200 GeV, for a small gluino lifetime, less than 3 hours. If the gluino lifetime is greater than 3 hours, the average efficiency of the trigger degrades because signal events are not recorded between accelerator stores. The resulting effect on the stopped gluino cross section limits for a χ_1^0 mass of 50 GeV is shown in Fig. 4.

This is the first search for exotic, out-of-time energy deposits at a high-energy collider. The results from 410 pb^{-1} of Tevatron data are able to exclude a cross section of about 1 pb for gluinos stopping in the D0 calorimeter and decaying to a gluon plus neutralino.

Thanks to Jay Wacker for very helpful inputs and discussions. We thank the staffs at Fermilab and collaborating institutions, and acknowledge support from the DOE and NSF (USA); CEA and CNRS/IN2P3 (France); FASI, Rosatom and RFBR (Russia); CAPES, CNPq, FAPERJ, FAPESP and FUNDUNESP (Brazil); DAE and DST (India); Colciencias (Colombia); CONACyT (Mexico); KRF and KOSEF (Korea); CONICET and UBACyT (Argentina); FOM (The Netherlands); PPARC (United Kingdom); MSMT (Czech Republic); CRC Program, CFI, NSERC and WestGrid Project (Canada); BMBF and DFG (Germany); SFI (Ireland); The Swedish Research Council (Sweden); Research Corporation; Alexander von Humboldt Foundation; and the Marie Curie Program.

[*] Visitor from Augustana College, Sioux Falls, SD, USA.
[§] Visitor from ICN-UNAM, Mexico City, Mexico.
[‡] Visitor from Helsinki Institute of Physics, Helsinki, Finland.
[#] Visitor from Universität Zürich, Zürich, Switzerland.

[1] N. Arkani-Hamed, S. Dimopoulos, G. F. Giudice, and A. Romanino, Nucl. Phys. B **709**, 3 (2005).
[2] G. R. Farrar and P. Fayet, Phys. Lett. B **76**, 575 (1978).
[3] A. Arvanitaki, S. Dimopoulos, A. Pierce, S. Rajendran and J. Wacker, arXiv:hep-ph/0506242.
[4] V. M. Abazov *et al.* [D0 Collaboration], Nucl. Instrum. Methods A **565**, 463 (2006).
[5] DØ Collaboration, S. Abachi *et al.*, Nucl. Instrum. Methods A **338**, 185 (1994).
[6] G. C. Blazey *et al.*, in *Proceedings of the Workshop: QCD and Weak Boson Physics in Run II,* edited by U. Baur, R. K. Ellis, and D. Zeppenfeld, Fermilab-Pub-00/297 (2000), Sec. 3.5.
[7] T. Sjöstrand *et al.*, Comp. Phys. Comm. **135**, 238 (2001).
[8] R. Brun and F. Carminati, CERN Program Library Long Writeup W5013, 1993 (unpublished).